NANO LETTERS

2008
Vol. 8, No. 7
2082-2086

# Atomic-Scale In-situ Observation of Carbon Nanotube Growth from Solid State Iron Carbide Nanoparticles

**Hideto Yoshida,[†,§] Seiji Takeda,[*,†,§] Tetsuya Uchiyama,[†,§] Hideo Kohno,[†,§] and Yoshikazu Homma[‡,§]**

*Graduate School of Science, Osaka University, 1-1 Machikane-yama, Toyonaka, Osaka 560-0043, Japan, Department of Physics, Tokyo University of Science, Shinjuku, Tokyo 162-8601, Japan, and CREST, Japan Science and Technology Agency, Chiyoda, Tokyo 102-0075, Japan*

*Received February 15, 2008; Revised Manuscript Received May 2, 2008*

## ABSTRACT

**We have first observed the nucleation and growth process of carbon nanotubes (CNTs) from iron carbide ($Fe_3C$) nanoparticles in chemical vapor deposition with $C_2H_2$ by in situ environmental transmission electron microscopy. Graphitic networks are formed on the fluctuating iron carbide nanoparticles, and subsequently CNTs are expelled from them. Our atomic scale observations suggest that carbon atoms diffuse through the bulk of iron carbide nanoparticles during the growth of CNTs.**

Carbon nanotubes (CNTs)[1,2] are regarded as one of the most important and promising materials for future nanotechnology. Their fascinating electronic properties can be varied from metal to semiconducting by their atomic structures.[3] Catalyst chemical vapor deposition (CVD) is now widely accepted as the best method for large scale production of CNTs.[4,5] Metal nanoparticles act as catalyst for the CVD growth, and recently the role played by nanoparticle catalysts (NPCs) has been revealed to some extent. However, no one has yet produced CNTs of desired atomic structures selectively. There have been a number of controversial hypotheses, theoretical simulations, and experiments on the growth process of CNTs. However, they have never been evaluated by direct observations at atomic scale. This has prevented us from understanding the growth process of CNTs convincingly and utilizing CNTs for electronic technology and industry. Crucial questions on the growth of CNTs are as follows. (1) Are NPCs liquid,[6,7] fluctuating crystalline,[8] or crystalline?[9] (2) Are NPCs carbide particles[6,10] or metal particles?[9,11,12] (3) Do carbon atoms migrate on the surface[9,13] and/or through the bulk[6] of NPCs? Here, we present atomic-scale in situ environmental transmission electron microscopy (ETEM)[9,14,15] observation of the nucleation of single-walled CNTs (SWNTs) and multiwalled CNTs (MWNTs) in Fe catalyzed CVD followed by continuous growth. Surprisingly, CNTs grow from NPCs of fluctuating crystalline Fe carbide. On the basis of this finding, we succeed in solving the long-standing questions without doubt.

Experimental procedure is summarized as follows. We deposited Fe (99.999%) of 1 nm thick on the thin $SiO_2$ surface layer of silicon substrates by vacuum evaporation. Some substrates were extremely tiny, so they were supported on carbon microgrids. The substrates were set in a newly designed ETEM (FEI Tecnai F20 equipped with an environmental-cell) operated at 200 kV. The substrates were heated to 600 °C in a vacuum, and subsequently, a mixture of $C_2H_2$:$H_2$ = 1:1 was introduced into the ETEM. The pressure of the gas and the temperature of the substrates in the CVD condition in the ETEM were 10 Pa and 600 °C, respectively. We have confirmed that ETEM images of CNTs in gases of such a low pressure are similar to those in vacuum.[16] As shown below, individual graphene layers are clearly visible in the CVD condition. ETEM images were recorded at a rate of 1 frame per 0.35 s using a CCD camera of 2048 × 2048 pixels. All of the images presented here are extracted from in situ ETEM observations.

First, we present the nucleation and growth process of both SWNTs (Figure 1a; Supporting Information S1) and MWNTs (Figure 2a; Supporting Information S2). Before the nucleation of a SWNT, a NPC exhibits different facets every frame, as shown in Figure 1a (e.g., $t$ = 8.05 and 16.45 s). Furthermore, various carbon cages protrude from the NPC frequently and disappear in a few seconds ($t$ = 5.25, 13.3, and 29.05 s). The shapes of both the unstable carbon cages and the NPC change rapidly (e.g., $t$ = 13.3 to 29.05 s). After the incubation

* Corresponding author. E-mail: takeda@tem.phys.sci.osaka-u.ac.jp.
† Osaka University.
‡ Tokyo University of Science.
§ CREST.

10.1021/nl080452q CCC: $40.75 
**Published on Web 05/28/2008**

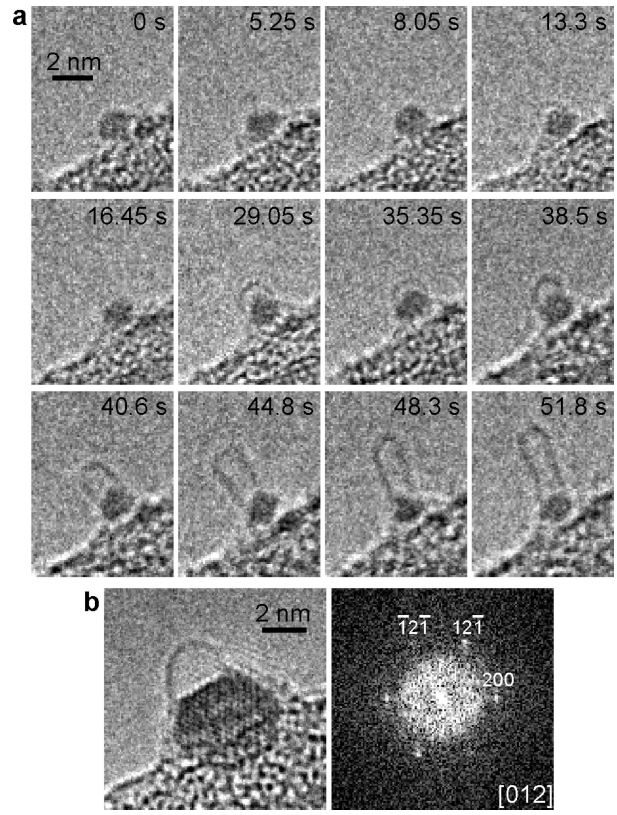


**Figure 1.** Nucleation and growth process of a SWNT from a NPC on a substrate. (a) Structural fluctuation of both carbon caps and a NPC is observed. The recording time is shown in images. (b) A snapshot of a NPC with a carbon dome. The NPC exhibits the lattice image and the corresponding extra diffraction in the Fourier transform. The NPC can be identified as Fe-carbide (cementite, $Fe_3C$) viewed along the [012] direction.

period, the stable dome, or the nucleus of a SWNT appears at $t = 35.35$ s. The nucleus grows gradually into a well-defined CNT of 1.5 nm in diameter and 3.6 nm long, as seen in Figure 1 (from $t = 40.6$ s to $t = 51.8$ s). From the images, we identify the CNT as a SWNT. After the nucleation of the SWNT, the NPC continues to fluctuate as suggested before.[8] In the nucleation process of a MWNT, graphene layers are first formed on a facet of a NPC, as seen in Figure 2a ($t = 0$ s). As is noted above, individual graphene layers can be clearly observed (see also Supporting Information S2). The graphene layers gradually extend and bend along the facets of the NPC ($t = 0.35$ s), and additional graphene layers nucleate beneath the existing ones. Accordingly, the NPC is gradually deformed ($t = 0.7$ s), forming the characteristic protrusion ($t = 2.1$ and 3.85 s). The NPC expels a MWNT suddenly, exhibiting the facet at the tip of its protrusion ($t = 4.9$ s), and this MWNT grows rapidly (from $t = 4.9$ to 5.95 s). Naturally, this root-grown MWNT is encapsulated at the tip.

We now show that NPCs are structurally fluctuating Fe-carbide. Figure 3 (Supporting Information S3) and Figure 4 (Supporting Information S4) show the root growth process of MWNTs viewed nearly normal to the growth direction and nearly end-on, respectively. In NPCs, various kinds of lattice images appear and fade out. For instance, the lattice image shown in Figure 3a−d continues for 1−2 s, 1−2 s,

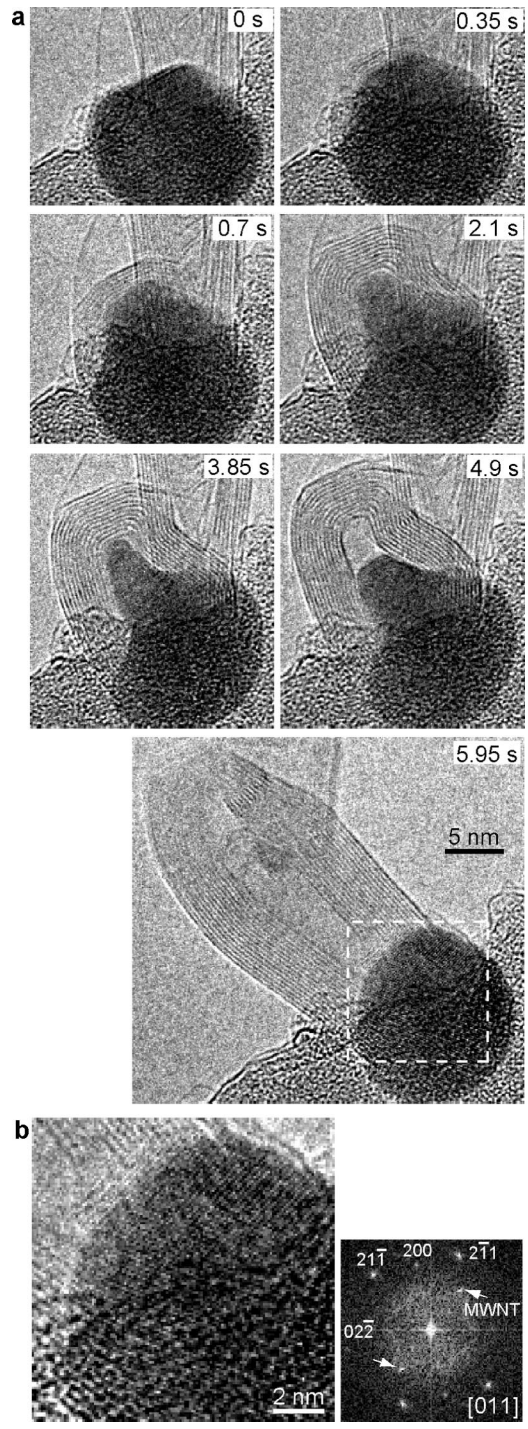


**Figure 2.** Nucleation and growth of a MWNT from a NPC on a substrate. (a) Graphene layers are formed on a NPC and then a MWNT is suddenly expelled from the deformed NPC. The recording time is shown in images. (b) The squared region of an image at 5.95 s in (a) is enlarged. The NPC exhibits the lattice image. The corresponding Fourier transform is also shown. The NPC can be identified as Fe-carbide (cementite, $Fe_3C$) viewed along the [011] direction. The spots by the MWNT are marked by the arrows.

1−2 s, and 7 s, respectively. Since the NPC remains at nearly the same position on the substrate and deforms only slightly as shown in Figure 3, the observed phenomenon is accounted for by a change in crystal orientation without physically rotating the whole NPC. We have found that all of the lattice

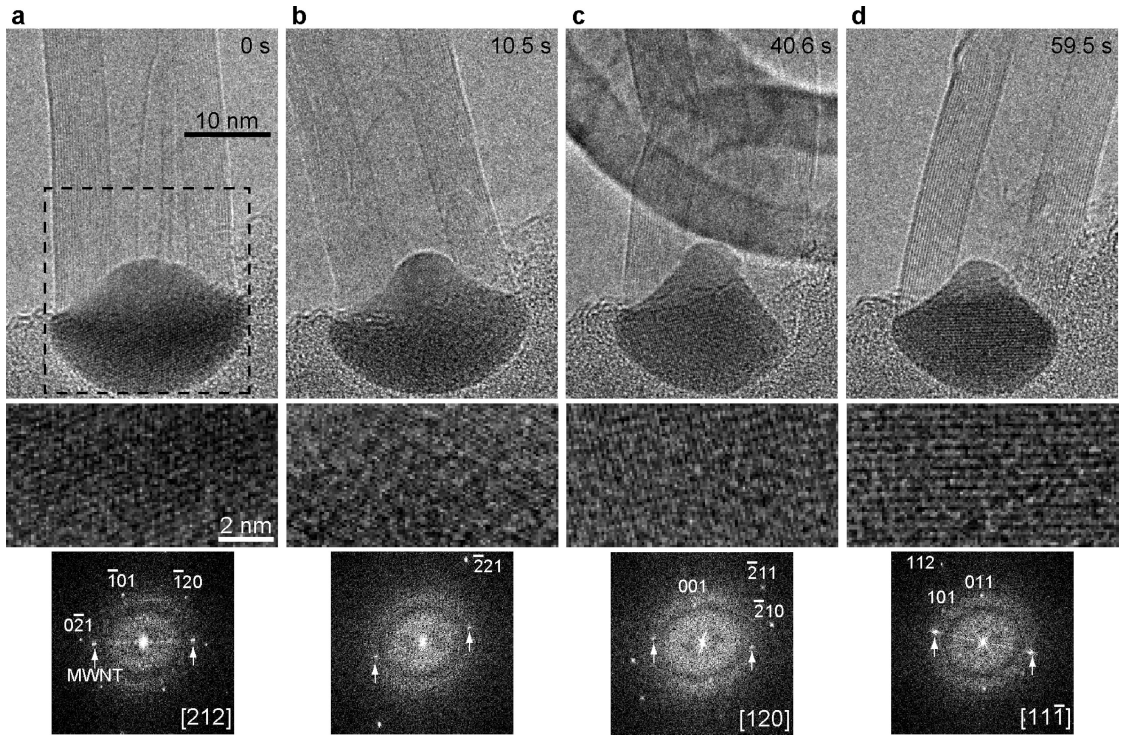


**Figure 3.** Growth process of a MWNT from an Fe carbide NPC viewed nearly normal to the growth direction. The recording time is shown in each image. Enlarged images and Fourier transforms of the dotted square regions in images are shown below. The spots by the MWNT are marked by the arrows.

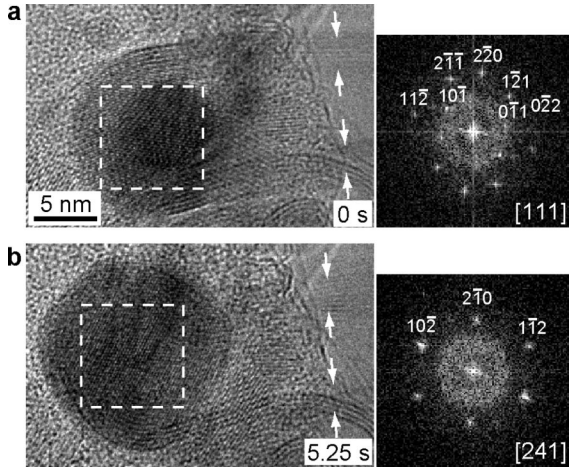


**Figure 4.** Growth of a MWNT from an Fe carbide NPC viewed nearly end-on. The recording time is shown in each image. Fourier transforms of the dotted square regions in images are also shown. Carbon walls which are slightly out of focus are indicated by a pair of arrows. Change in size of the NPC in (a) and (b) is simply attributed to the deformation of NPCs, as seen in Figure 3.

images in Figure 3 and Figure 4 are consistently explained by neither pure iron α(bcc) nor γ(fcc) structures but the iron-carbide structure, that is, cementite, $Fe_3C$.[17] As shown in Fourier transform of lattice image in Figure 3 and Figure 4, we can index the diffraction spots based on the cementite structure. Estimated interplanar angles agree well with those measured in the observations within the accuracy of 2% in Figure 3a,c,d and 1% in Figure 4. Crystal orientation changes significantly, for instance, by 49.3° from Figure 3a to Figure 3c and 32.2° from Figure 3c to Figure 3d. Lattice image in another series of observation (Figure 2b) can also be explained by the cementite structure. The structure of smaller NPCs for the growth of SWNTs seems to fluctuate more remarkably. The observed interplanar angles of the cementite structure in Figure 1b change by 0.3−5.6% from frame to frame. It is well-known that metal nanoparticles fluctuate in vacuum at room temperature.[18–20] We think that the nanoparticles of cementite, which is known to be hard and brittle in iron steels, fluctuate not in vacuum but only under the gas environment at the elevated temperature. It is noteworthy that the growth of CNTs never be interrupted by the structural fluctuation of carbide NPCs (see Supporting Information S3). It is also pointed out that NPCs deform slowly and slightly, as revealed in Figure 3 (Supporting Information S3). The deformation of NPCs gives rise to the swing of CNTs, which has already been observed by ETEM.[21] There seems no apparent correlation between the deformation of NPCs and the change in the crystal orientation of NPCs. The deformation likely originates from some disturbance to growth such as local imbalance of the absorption rate of carbon into a NPC and the desorption rate of carbon from the NPC to a part of a CNT.

From the key observations mentioned above, we can now clear the controversial growth process of CNTs in Fe catalyzed CVD condition as follows. (1) NPCs are fluctuating crystalline nanoparticles and (2) the NPCs are carbide, that is, cementite $Fe_3C$. In addition, we strongly suggest that (3) carbon atoms migrate through NPC bulk. We explain this suggestion as follows. We have observed that all of the graphene cylinders of different diameter in a MWNT grow at the same growth rate (Supporting Information S3). Since

the growth rate of a graphene cylinder is most probably determined by the sticking rate of carbon atoms to the open end of the graphene cylinder, or the interface between the graphene cylinder and the NPC, the observation indicates that carbon density is homogeneous at all ends. Hence, it is most likely that carbon atoms, supplied on the open surface of the NPC from the gas, migrate toward the open ends through the NPC rather than the interface and/or the surface of the NPC. Any instantaneous carbide crystal in a NPC probably includes a certain amount of lattice vacancies as a bulk crystal near its melting temperature, so carbon atoms can migrate via the vacancy mechanism of self-diffusion through the NPC. In other words, volume diffusion is dominant, in particular in the growth of MWNTs.

Here, we discuss previous works in the light of our study. Baker et al.[22] speculated that metal (Ni) particle catalysts for the growth of carbon filaments or carbon fibers have a property of liquid and that they reshape and lift from a substrate, expelling carbon filaments beneath themselves (Figure 5 of ref 22). Many works followed the "liquid-like" metal NPCs for the growth of CNTs. Hofmann et al.[8] have claimed by ETEM observation that a SWNT is grown from "liquid-like" metal (Ni) NPCs or fluctuating Ni crystal NPCs, even though it is unclear that their observation really represents the growth process of CNTs. The mechanism proposed by Baker et al. is common to the vapor−liquid−solid (VLS) growth mechanism for silicon whiskers[23,24] or silicon nanowires, in which gold particles act as catalyst. During VLS growth, gold particles absorb silicon and become liquid particles of gold and silicon. This is simply interpreted by the fact that the eutectic temperature of the Au and Si binary system, that is, 363 °C, is sufficiently lower than the growth temperature of silicon nanowires, typically around 500 °C. Kodambaka et al.[25] have reported that germanium nanowires grow below the eutectic temperature. On the other hand, the growth temperature of carbon nanofilaments as well as CNTs are much lower than the melting temperatures in binary bulk systems of C and Fe or other catalyst metals such as Ni and Co. Therefore, the hypothesis of liquid-like NPCs has long been controversial. Structural data about nanoparticles not during but after CVD growth have been accumulated by transmission electron microscopy. Several authors identified carbide nanoparticles such as $Ni_3C$ in CNTs[26] and $Fe_3C$ in both CNTs[27] and carbon fibers[28] in addition to metal (Fe, Ni, and Co) nanoparticles. By means of in situ X-ray diffraction, Emmenegger et al.[10] have studied the structures of NPCs in Fe catalyzed CVD. They have concluded that the structure of NPCs is iron carbide ($Fe_3C$). However, X-ray studies can only reveal spatially averaged structures of NPCs and have never shown the dynamic structures of individual NPCs at atomic scale. Therefore, our direct ETEM observation has elucidated the controversial "liquid-like NPCs" to great extent. Dai and others[4] proposed a nucleation mechanism of CNTs in catalyst CVD, the yarmulke mechanism, so-called. Carbon atoms, absorbed on the surface of a NPC, agglomerate and form a carbon cap in order to diminish surface energy of the NPC. Subsequently, the cap is grown and lifted from the NPC, forming an encapsulated CNT. Several authors attempted to reproduce the nucleation of CNTs by molecular dynamics (MD) simulations. Shibuta and Maruyama[29] reported that, after a hexagonal carbon network covers the surface of a free-standing crystalline metal (Ni) cluster, further supply of carbon leads to a hump of carbon network. Gavillet et al.[30] discussed the nucleation mechanism based on more elaborate quantum MD simulations. They suggested that the segregation of carbon linear chains and atomic rings on the surface of a liquid-like carbon−metal (Co) cluster is the first stage of the nucleation process. Since MD simulations can reproduce a process only for a short period, that is, picoseconds to several hundreds of nanoseconds, it is unclear that these simulated precursors of carbon actually grow into CNTs. Our ETEM observation has indicated that CNTs nucleate via complex dynamic motion of constituent metal and carbon atoms in carbide NPCs and that the yarmulke mechanism is oversimplified.

We mention briefly the possibility of the structural control of CNTs. Structural fluctuation of NPCs is more enhanced when they are smaller (Figure 1). In this respect, the structural control of SWNTs seems more difficult. However, our observation in Figure 1 reads that the structural fluctuation of NPCs on substrates is needed until NPCs become the proper atomistic structure that leads to the nuclei of SWNTs. Therefore, we suggest that the structural control of SWNTs is possible by preparing NPCs with the proper structures on substrates. New kinds of catalysts have been found such as gold, silicon, and silicon carbide.[31,32] The NPCs with the proper structures, in particular, silicon carbide, may potentially be fabricated on crystalline substrates via epitaxial growth techniques. Therefore, our direct ETEM observation has now directed the possible routes for the structural control of CNTs.

In summary, our atomic-scale in situ observation of Fe catalyzed CVD growth of CNTs has shown that iron carbide ($Fe_3C$) nanoparticles act as catalyst. Iron carbide ($Fe_3C$) NPCs fluctuate structurally in the CVD condition. Volume diffusion of carbon in carbide NPCs is very likely. These finding may bring general understanding of catalyzed CVD growth of CNTs at atomic scale. It may bring further implications for the structural control of CNTs, for instance, by preparing structurally well-controlled carbide NPCs on a crystalline substrate via epitaxial growth.

**Acknowledgment.** We thank Yusuke Tanemoto for preparing silicon substrates.

**Supporting Information Available:** ETEM movies showing the nucleation and growth of CNTs. This material is available free of charge via the Internet at http://pubs.acs.org.

## References

(1) Iijima, S. *Nature* **1991**, *354*, 56.
(2) Iijima, S.; Ichihashi, T. *Nature* **1993**, *363*, 603.
(3) Hamada, N.; Sawada, S.; Oshiyama, A. *Phys. Rev. Lett.* **1992**, *68*, 1579.
(4) Dai, H.; Rinzler, A. G.; Nikolaev, P.; Thess, A.; Colbert, D. T.; Smalley, R. E. *Chem. Phys. Lett.* **1996**, *260*, 471.
(5) Hata, K.; Futaba, D. N.; Mizuno, K.; Namai, T.; Yumura, M.; Iijima, S. *Science* **2004**, *306*, 1362.
(6) Homma, Y.; Kobayashi, Y.; Ogino, T.; Takagi, D.; Ito, R.; Jung, Y. J.; Ajayan, P. M. *J. Phys. Chem. B* **2003**, *107*, 12161.

(7) Harutyunyan, A. R.; Mora, E.; Tokune, T.; Bolton, K.; Rosén, A.; Jiang, A.; Awasthi, N.; Curtarolo, S. *Appl. Phys. Lett.* **2007**, *90*, 163120.
(8) Hofmann, S.; Sharma, R.; Ducati, C.; Du, G.; Mattevi, C.; Cepek, C.; Cantoro, M.; Pisana, S.; Parvez, A.; Cervantes-Sodi, F.; Ferrari, A. C.; Dunin-Borkowski, R.; Lizzit, S.; Petaccia, L.; Goldoni, A.; Robertson, J. *Nano Lett.* **2007**, *7*, 602.
(9) Helveg, S.; López-Cartes, C.; Sehested, J.; Hansen, P. L.; Clausen, B. S.; Rostrup-Nielsen, J. R.; Ablid-Pedersen, F.; Nørskov, J. K. *Nature* **2004**, *427*, 426.
(10) Emmenegger, C.; Bonard, J.-M.; Mauron, P.; Sudan, P.; Lepora, A.; Grobety, B.; Züttel, A.; Schlapbach, L. *Carbon* **2003**, *41*, 539.
(11) Jung, Y. H.; Wei, B.; Vajtai, R.; Ajayan, P. M.; Homma, Y.; Prabhakaran, K.; Ogino, T. *Nano Lett.* **2003**, *3*, 561.
(12) Lin, M.; Tan, J. P. Y.; Boothroyd, C.; Loh, K. P.; Tok, E. S.; Foo, Y.-L. *Nano Lett.* **2006**, *6*, 449.
(13) Hofmann, S.; Csányi, G.; Ferrari, A. C.; Payne, M. C.; Robertson, J. *Phys. Rev. Lett.* **2005**, *95*, 036101.
(14) Sharma, R.; Iqbal, Z. *Appl. Phys. Lett.* **2004**, *84*, 990.
(15) Boyes, E. D.; Gai, P. L. *Ultramicroscopy* **1997**, *67*, 219.
(16) Yoshida, H.; Takeda, S. *Phys. Rev. B* **2005**, *72*, 195428.
(17) Villars, P.; Calvert, L. D. *Pearson's handbook of crystallographic data for intermetallic phases*; American Society for Metals, 1985.
(18) Iijima, S.; Ichihashi, T. *Phys. Rev. Lett.* **1986**, *56*, 616.
(19) Marks, L. D. *Rep. Prog. Phys.* **1994**, *57*, 603.
(20) Be'er, A.; Kofman, R.; Phillipp, F.; Lereah, Y. *Phys. Rev. B* **2006**, *74*, 224111.
(21) Yoshida, H.; Uchiyama, T.; Takeda, S. *Jpn. J. Appl. Phys.* **2007**, *46*, L917.
(22) Baker, R. T. K.; Barber, M. A.; Harris, P. S.; Feates, F. S.; Waite, R. J. *J. Catal.* **1972**, *26*, 51.
(23) Wagner, R. S.; Ellis, W. C. *Appl. Phys. Lett.* **1964**, *4*, 89.
(24) Ozaki, N.; Ohno, Y.; Takeda, S. *Appl. Phys. Lett.* **1998**, *73*, 3700.
(25) Kodambaka, S.; Tersoff, J.; Reuter, M. C.; Ross, F. M. *Science* **2007**, *316*, 729.
(26) Arie, T.; Nishijima, H.; Akita, S.; Nakayama, Y. *J. Vac. Sci. Technol. B* **2000**, *18*, 104.
(27) Yoshida, N.; Yasutake, M.; Arie, T.; Akita, S.; Nakayama, Y. *Jpn. J. Appl. Phys.* **2002**, *41*, 5013.
(28) Oberlin, A.; Endo, M.; Koyama, T. *J. Cryst. Growth* **1976**, *32*, 335.
(29) Shibuta, Y.; Maruyama, S. *Chem. Phys. Lett.* **2003**, *382*, 381.
(30) Gavillet, J.; Loiseau, A.; Journet, C.; Willaime, F.; Ducastelle, F.; Charlier, J.-C. *Phys. Rev. Lett.* **2001**, *87*, 275504.
(31) Takagi, D.; Homma, Y.; Hibino, H.; Suzuki, S.; Kobayashi, Y. *Nano Lett.* **2006**, *6*, 2642.
(32) Takagi, D.; Hibino, H.; Suzuki, S.; Kobayashi, Y.; Homma, Y. *Nano Lett.* **2007**, *7*, 2272.

NL080452Q